A Specialized Forebrain Circuit for Vocal Babbling in the Juvenile Songbird

Dmitriy Aronov, Aaron S. Andalman, Michale S. Fee*

Young animals engage in variable exploratory behaviors essential for the development of neural circuitry and adult motor control, yet the neural basis of these behaviors is largely unknown. Juvenile songbirds produce subsong—a succession of primitive vocalizations akin to human babbling. We found that subsong production in zebra finches does not require HVC (high vocal center), a key premotor area for singing in adult birds, but does require LMAN (lateral magnocellular nucleus of the nidopallium), a forebrain nucleus involved in learning but not in adult singing. During babbling, neurons in LMAN exhibited premotor correlations to vocal output on a fast time scale. Thus, juvenile singing is driven by a circuit distinct from that which produces the adult behavior—a separation possibly general to other developing motor systems.

How does a young brain learn to use the muscles it controls and the sensory organs by which it perceives the world? To a surprising extent, this knowledge is not built in by deterministic developmental rules but must be obtained through exploration. For instance, the relationship between feedback from the somatosensory periphery and movement is revealed to the developing brain by spontaneous muscle twitches, which facilitate the self-organization of spinal reflex circuits (*1*) and cortical somatosensory maps (*2*, *3*). At a higher level, juvenile animals learn the causal relation between actions and the effects of these actions by producing highly variable behaviors such as infant stepping, grasp-like "hand babbling," early vocalizations, and play (*4*–*8*).

How are these exploratory juvenile behaviors generated? Are they produced by the same brain areas responsible for the corresponding adult behaviors later in life, or are specialized brain regions involved? Forebrain areas, including the motor cortex and the basal ganglia, have been implicated in the production of normal infant movements, as well as their abnormalities (*5*, *9*–*11*). Yet the specific forebrain circuits for infant motor control remain to be identified.

Babbling is an early motor behavior produced by juveniles of vocal mammals and birds (*6*, *12*–*15*). In zebra finches, babbling, called subsong, occurs roughly from ages 30 to 45 days post-hatch (dph). Plastic song follows, with the gradual appearance of distinct and identifiable, but variable, vocal elements (syllables). By 80 to 90 dph, plastic song is gradually transformed into highly complex, stereotyped motifs—sequences of syllables that constitute adult song. The premotor circuit for adult song production consists of HVC (high vocal center), RA (robust nucleus of the arcopallium), and brainstem motor nuclei (Fig. 1A). This "motor pathway" is crucial for generating stereotyped, learned vocalizations (*16*, *17*) and exhibits firing that is precisely time-locked to the song output (*18*–*21*).

Another circuit, the anterior forebrain pathway (AFP), is homologous to basal ganglia thalamocortical loops in mammals and projects to RA through a forebrain nucleus, LMAN (lateral magnocellular nucleus of the nidopallium) (*22*, *23*). Although LMAN is not required for singing in adult birds, it is necessary for normal song learning in juveniles (*24*, *25*) and plays a role in producing song variability in adult and juvenile birds (*26*, *27*). These and other studies have suggested a view that the motor pathway drives singing, whereas the output of the AFP modulates or instructs the motor pathway during learning (*28*, *29*).

Subsong persists in the absence of HVC. We investigated whether primitive subsong vocalizations result from an immature form of the adult motor pathway, or whether they are driven by other premotor circuits. Given the importance of HVC for mature singing (*16*, *20*, *30*), we sought to characterize its involvement early in development. In nine subsong-producing juvenile birds (ages 33 to 44 dph), we eliminated HVC bilaterally, either by electrolytic lesions or by pharmacological inactivation (*31*). In three additional birds, we left HVC intact but specifically eliminated its projection to RA by bilateral transection of the HVC-to-RA fiber tract. After these manipulations, all birds continued producing largely unaffected subsong (Fig. 1A and fig. S3).

Surprisingly, older birds—those in the plastic-song stage (45 to 73 dph, $n = 12$) and adults ($n = 5$, undirected singing)—also sang after bilateral HVC elimination [but see (*31*)]. These birds lost structure and stereotypy in their songs, reverting to the production of subsong-like vocalizations. After pharmacological inactivation of HVC, this reversion to subsong-like vocalizations was fast (within 20 min) and reversible (fig. S4); this finding suggested that the effect is not due to long-term changes in neural circuitry, but rather occurs immediately as a result of the loss of spiking activity in HVC. At all ages, singing in the absence of HVC was produced at normal rates and followed an ordinary circadian rhythm, with more songs produced in the morning than in later parts of the day (*31*).

Singing without HVC is highly similar to normal subsong. We asked whether the sounds produced in the absence of HVC were indeed similar to subsong. We characterized acoustic properties of songs by measuring spectral features shown to be effective for quantifying developmental trends in zebra finches (*32*, *33*). Distributions of these features before and after HVC elimination were highly similar for subsong-producing birds (*31*). An additional feature of normal subsong is the absence of repeatable acoustic elements of a stereotyped length. This was evident in a wide, unimodal distribution of syllable durations for subsong-producing birds ($n = 9$ birds younger than 45 dph; Fig. 2, A and B). After HVC elimination, these distributions were unchanged (*31*). In contrast, plastic and adult songs contain distinct syllables that form multiple narrow peaks in the distributions of durations. After HVC elimination in older birds, all distinct syllables were lost, resulting in unimodal distributions similar to those of subsong ($n = 25$ birds) (*31*).

Furthermore, subsong is characterized by a lack of sequential stereotypy, which appears later in plastic and adult songs. We quantified stereotypy by measuring the peak of the spectral cross-correlation between different song renditions (Fig. 2C) (*31*). In control conditions, stereotypy was higher for older birds (Fig. 2D; $P < 0.0001$ for nonzero slope of the linear regression of stereotypy and age). However, independently of age, stereotypy was reduced to the level of subsong after HVC elimination (Wilcoxon $P > 0.1$ for the difference from normal subsong). In summary, analyses of acoustic structure indicate that, by a wide range of measurements, singing in the absence of HVC is highly similar to normal subsong.

Subsong requires activity in RA and LMAN. If subsong persists in the absence of HVC, what neural circuits are engaged in its production? One possibility is that subsong does not require the forebrain song system and is entirely produced by midbrain or brainstem circuitry, even in the absence of RA. A second possibility is that subsong is driven by circuitry intrinsic to RA, even in the absence of HVC and LMAN. The third possibility is that subsong is driven by, or requires, inputs from LMAN to RA. We tested

McGovern Institute for Brain Research, Department of Brain and Cognitive Sciences, Massachusetts Institute of Technology, Cambridge, MA 02139, USA.

*To whom correspondence should be addressed. E-mail: fee@mit.edu

these hypotheses by lesions and inactivations of RA and LMAN.

RA lesions entirely blocked singing in juvenile birds (n = 5, 39 to 73 dph), indicating that subsong-like vocalizations require descending inputs from the forebrain (Fig. 3). Similarly, song production was abolished by lesions of HVC and subsequent inactivation of LMAN (n = 12 experiments in 5 birds, 51 to 75 dph), indicating that RA circuitry, without its afferent inputs, is not sufficient to generate singing. We further tested the necessity of LMAN inputs to RA by inactivating LMAN in juvenile birds. LMAN inactivation entirely abolished subsong production in all birds younger than 45 dph (n = 6 experiments in 4 birds). However, in agreement with previous studies, LMAN inactivation did not block singing in most older birds (6 of 7 experiments in 5 birds, 45 to 67 dph), although it produced a marked reduction in song variability (*26*, *27*). Together, these results indicate that RA and its inputs from LMAN are necessary for subsong production.

LMAN neurons exhibit premotor activity during subsong. An intriguing possibility suggested by the above results is that LMAN drives subsong production—i.e., that it generates patterns of spiking activity that control the acoustic structure of subsong on a short (10 ms) time scale. To test this prediction directly, we recorded from single RA-projecting LMAN neurons during subsong production in intact birds [n = 15 neurons in 3 birds, 38 to 45 dph (*31*)] and in birds with bilateral HVC lesions (n = 16 neurons in 2 birds, lesioned at 38 and 50 dph). To quantify premotor activity, we examined firing in a short window preceding each syllable boundary (onset or offset). To begin with, we only considered syllable boundaries separated from other onsets or offsets by relatively long (>150 ms) periods to eliminate the possible confounding effects of neighboring syllables on the firing pattern. There was a significant increase in firing before syllable onsets in 12 of 31 neurons [16.1 ± 1.6 Hz in a 50-ms window preceding syllable onset versus 8.6 ± 0.6 Hz in a 100-ms baseline period preceding this window; $P < 0.05$; e.g., neuron 3, Fig. 4, A and B (*31*)]. Similarly, syllable offsets were preceded by a significant increase in firing in 5 of 31 neurons (21.2 ± 3.4 Hz before syllable offset versus baseline, 15.5 ± 1.3 Hz; $P < 0.05$; e.g., neuron 14, Fig. 4, C and D). Similar neuronal firing patterns related to onsets and offsets of behavioral sequences have been observed in other basal ganglia–related circuits (*34*).

In the above analysis, we only considered syllable boundaries separated by long (>150 ms) periods of time to isolate syllable onset- and offset-related changes in firing. However, the firing of some LMAN neurons also correlated with more rapid changes in song structure. For instance, neuron 12 (Fig. 4, E to G) exhibited increased firing before syllables that followed short (10 to 150 ms) rather than long intervals, as well as a reduction in firing during silent periods between syllables. Overall, seven neurons showed a premotor increase in activity before syllables separated by short intervals ($P < 0.05$ for the comparison of a 30-ms window preceding a syllable with 30 ms of baseline). This finding suggests that some LMAN neurons may have a premotor relation to subsong structure at the level of individual syllables.

In neurons that exhibited a significant increase in firing before syllable onsets (n = 18),

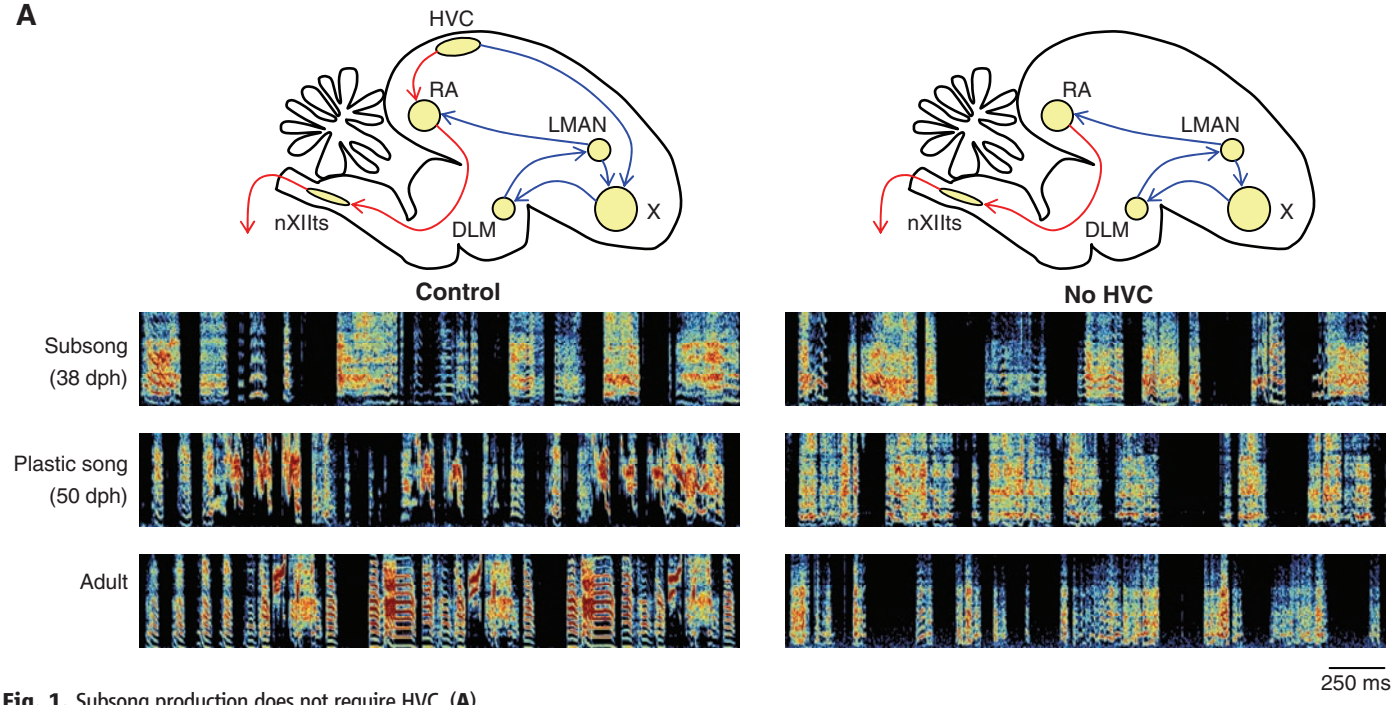

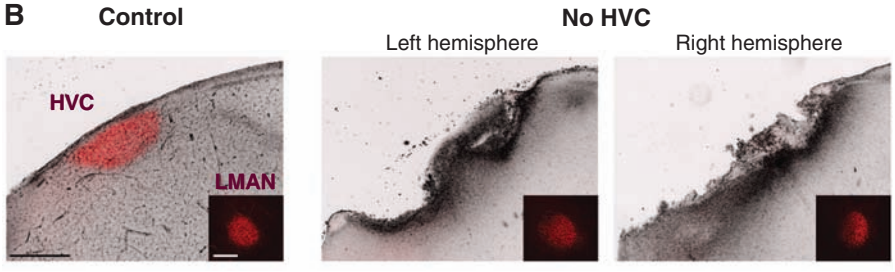

Fig. 1. Subsong production does not require HVC. (**A**) Results of bilateral HVC elimination (by lesion or pharmacological inactivation). Top: major connections of the song system with and without HVC. Red, motor pathway; blue, anterior forebrain pathway (AFP); X, area X, a basal-ganglia homolog; DLM, dorsolateral nucleus of the anterior thalamus; nXIIts, tracheosyringeal portion of the hypoglossal nucleus. Lower left: Sonograms of three birds at different ages. Lower right: Sonograms of the same birds in the absence of HVC. Frequency ranges from 500 Hz to 7.5 kHz; color scale (from black to red) spans a power range of 8 dB. For audio clips of these songs, see (*31*). (**B**) Histological verification of HVC lesions. Left: Inverted dark-field image of a parasagittal section of a normal zebra finch brain (50 dph). Red indicates retrograde fluorescence labeling of neurons in HVC after tracer (Alexa-conjugated cholera toxin subunit β) injection into RA. Inset: retrograde labeling of neurons in LMAN from the same injection. Right: Brain sections of the plastic-song bird shown in (A). Scale bars, 500 μm.

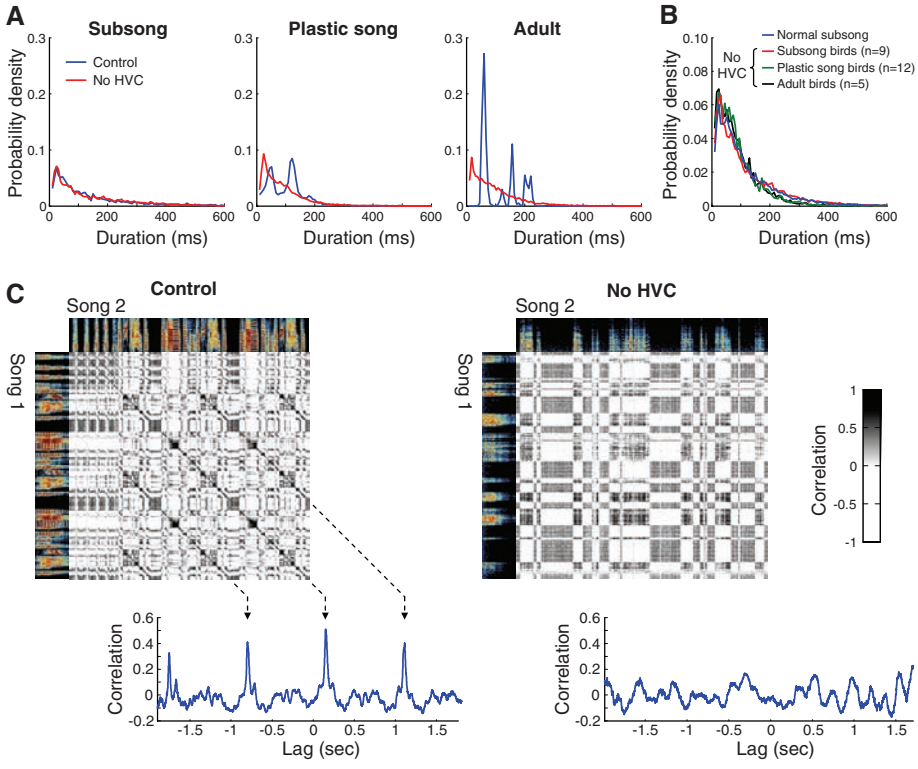

Fig. 2. Singing in the absence of HVC is highly similar to normal subsong. (**A**) Distributions of syllable durations for three birds of various ages (blue) and distributions for the same birds in the absence of HVC (red). (**B**) Average syllable duration distributions for normal subsong-producing birds (blue) and birds of different ages in the absence of HVC. (**C**) Sample spectral correlation matrices for a pair of songs produced by an adult bird (left) and by the same bird after HVC lesion (right). Averaging the matrix along its diagonals reveals strong correlation peaks in control (pre-lesion) condition, but not after HVC lesion. (**D**) Maximum values of the spectral correlation, averaged across all pairwise comparisons of 10 song bouts (*31*), for birds in control conditions and for the same birds in the absence of HVC. Dashed lines, linear regression; error bars, SEs across all 45 pairwise comparisons.

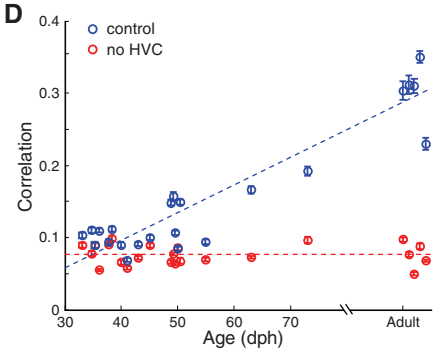

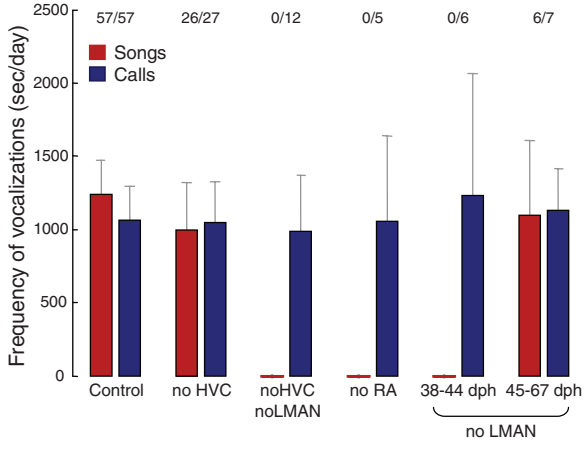

Fig. 3. Subsong production requires LMAN and RA. Average rates of song and call production in all lesion and inactivation experiments are shown. For rate measurement, a full day of recording was partitioned into 1-s segments, and the numbers of segments containing calls or songs were estimated (*31*). In cases where age is unspecified, data from all birds are pooled together. Note that for subsong-producing birds (<45 dph), the average rate of singing was not affected by HVC elimination (Wilcoxon $P > 0.5$). LMAN lesions in older juveniles (rightmost group) resulted in highly stereotyped song (*27*). Values at top are fractions of experiments in which any amount of singing occurred. Error bars are SEM values across birds. In experiments that abolished singing, silencing was specific to songs and did not affect the frequency of call vocalizations that are known not to require the song system (*17*).

high-frequency bursts of spikes (>100 Hz) preceded 13.2 ± 1.4% of syllables. The most likely timing of a burst onset was 17.2 ± 3.1 ms before syllable onset. Such latency is, in fact, anticipated for premotor activity in LMAN, given the 10- to 15-ms latency reported for vocal perturbation after electrical stimulation in RA (*35*) and the 2- to 5-ms antidromic latency from RA we found in LMAN neurons (*31*). Note that although the exact relationship of firing to song varied across cells, 20 of 31 neurons we recorded (65%) showed some type of premotor correlation to the vocal output. Premotor firing in LMAN did not require activity within HVC; 8 of 16 neurons exhibited significant correlations to song structure in HVC-lesioned birds (fig. S5).

Discussion. Our data indicate that LMAN, and possibly other components of the AFP, constitute an essential premotor circuit for the production of early babbling. At the same time, we have shown that the classical premotor nucleus HVC (*16*) is not necessary for the generation of subsong. We therefore propose that two premotor pathways in the songbird function to produce vocalizations at different stages of development. In young juveniles, the AFP generates poorly structured subsong, whereas in adult birds, the classical HVC-motor pathway generates highly stereotyped motor sequences. These pathways interact in the intermediate plastic-song stage (*27*) to generate the partially structured but variable vocalizations upon which vocal learning operates.

The transfer of functional dominance from one pathway to another during vocal learning elegantly parallels their anatomical development. HVC does not reach its adult size until the late plastic-song stage (*36*) and establishes functional synapses in RA later than LMAN does (*37*, *38*). Song maturation and the decrease in vocal variability have thus been attributed to the strengthening of inputs from HVC and the concurrent weakening of inputs from LMAN (*39*–*42*). Curiously, although HVC neurons form synapses in RA around the onset of singing [30 to 35 dph (*37*)], our results show that they do not significantly contribute to song production in its earliest stage. It is therefore possible that the HVC-to-RA pathway is active during early subsong but is not yet functionally strong enough to drive singing by itself or to influence vocalizations in a detectable way.

Identifying forebrain circuits involved in the production of juvenile behaviors is a requisite step toward understanding the mechanisms by which sensorimotor learning takes place. Several models of developmental learning suggest that early motor behaviors originate in the same circuits that later produce adult behavior. In this view, known as neuronal group selection theory, an initially large number of motor patterns undergo a selection process through competition, gradually eliminating circuits that produce undesirable behaviors (*9*, *43*–*46*). Our findings, however, suggest a rather different model in which distinct specialized circuits are dedicated to the

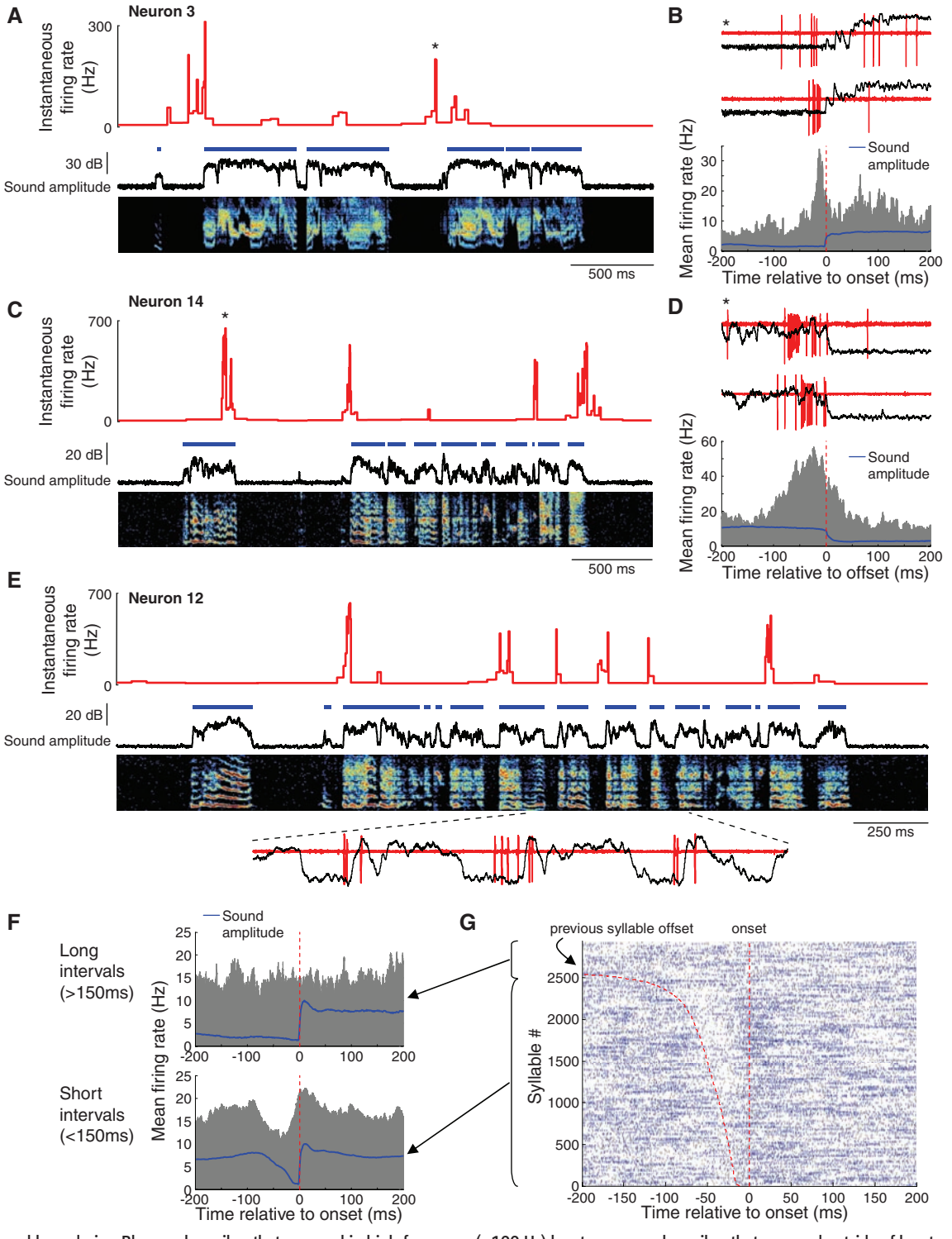

Fig. 4. LMAN exhibits premotor activity during subsong. (**A**) Activity of an RA-projecting LMAN neuron during subsong production. Blue segments indicate individual syllables. Instantaneous firing rate exhibits peaks before syllable onsets. (**B**) Examples of spiking activity (red) before onset of sound amplitude (black) for neuron 3. Asterisk indicates a matching example with (A). Histograms show average firing rate across all syllable onsets for neuron 3; blue trace, average sound amplitude. Average includes only those syllables that were preceded by long (>150 ms) periods of silence. (**C** and **D**) Activity of a neuron that exhibited peaks in firing before syllable offsets, plotted as in (A) and (B). Averages in (D) include only long (>150 ms) syllables that were followed by long (>150 ms) periods of silence in order to isolate offset-related changes in firing from onset-related changes. (**E**) Activity of a neuron that exhibited firing before syllable onsets after short (<150 ms) intervals, plotted as in (A). Bottom: Spiking activity (red) occurring before syllable onsets for neuron 12. (**F**) Averages of firing rate and sound amplitude for neuron 12, separately for syllables that followed short (10 to 150 ms) and long (>150 ms) intervals, plotted as in (B). (**G**) Syllable onset–centered spike raster for neuron 12. Raster is sorted according to the length of the interval that preceded the syllables; dashed lines indicate interval boundaries. Blue marks, spikes that occurred in high-frequency (>100 Hz) bursts; gray marks, spikes that occurred outside of bursts.

generation of highly variable juvenile behavior. We speculate that similar circuits for the production of infant behavior may be a general feature of developmental learning in the vertebrate brain.

References and Notes

1. P. Petersson, A. Waldenstrom, C. Fahraeus, J. Schouenborg, *Nature* **424**, 72 (2003).
2. R. Khazipov *et al.*, *Nature* **432**, 758 (2004).
3. M. Milh *et al.*, *Cereb. Cortex* **17**, 1582 (2007).
4. P. S. Wallace, I. Q. Whishaw, *Neuropsychologia* **41**, 1912 (2003).
5. S. R. Robinson, M. S. Blumberg, M. S. Lane, L. A. Kreber, *Behav. Neurosci.* **114**, 328 (2000).
6. A. J. Doupe, P. K. Kuhl, *Annu. Rev. Neurosci.* **22**, 567 (1999).
7. T. Imada *et al.*, *Neuroreport* **17**, 957 (2006).
8. R. Fagen, *Animal Play Behavior* (Oxford Univ. Press, New York, 1981).
9. H. Forssberg, *Curr. Opin. Neurobiol.* **9**, 676 (1999).
10. J. A. Eyre, S. Miller, G. J. Clowry, E. A. Conway, C. Watts, *Brain* **123**, 51 (2000).
11. H. F. Prechtl *et al.*, *Lancet* **349**, 1361 (1997).
12. P. Marler, *Am. Sci.* **58**, 669 (1970).
13. A. M. Elowson, C. T. Snowdon, C. Lazaro-Perea, *Trends Cogn. Sci.* **2**, 31 (1998).
14. M. Knornschild, O. Behr, O. von Helversen, *Naturwissenschaften* **93**, 451 (2006).
15. D. Reiss, B. McCowan, *J. Comp. Psychol.* **107**, 301 (1993).
16. F. Nottebohm, T. M. Stokes, C. M. Leonard, *J. Comp. Neurol.* **165**, 457 (1976).
17. H. B. Simpson, D. S. Vicario, *J. Neurosci.* **10**, 1541 (1990).

18. A. C. Yu, D. Margoliash, *Science* **273**, 1871 (1996).
19. Z. Chi, D. Margoliash, *Neuron* **32**, 899 (2001).
20. R. H. Hahnloser, A. A. Kozhevnikov, M. S. Fee, *Nature* **419**, 65 (2002).
21. A. Leonardo, M. S. Fee, *J. Neurosci.* **25**, 652 (2005).
22. S. W. Bottjer, K. A. Halsema, S. A. Brown, E. A. Miesner, *J. Comp. Neurol.* **279**, 312 (1989).
23. M. A. Farries, D. J. Perkel, *J. Neurosci.* **22**, 3776 (2002).
24. S. W. Bottjer, E. A. Miesner, A. P. Arnold, *Science* **224**, 901 (1984).
25. C. Scharff, F. Nottebohm, *J. Neurosci.* **11**, 2896 (1991).
26. M. H. Kao, A. J. Doupe, M. S. Brainard, *Nature* **433**, 638 (2005).
27. B. P. Ölveczky, A. S. Andalman, M. S. Fee, *PLoS Biol.* **3**, e153 (2005).
28. K. Doya, T. J. Sejnowski, in *Advances in Neural Information Processing Systems*, G. Tesauro, D. S. Tourezky, T. K. Leen, Eds. (MIT Press, Cambridge, MA, 1995), vol. 7, pp. 101–108.
29. T. W. Troyer, S. W. Bottjer, *Curr. Opin. Neurobiol.* **11**, 721 (2001).
30. J. A. Thompson, F. Johnson, *Dev. Neurobiol.* **67**, 205 (2007).
31. See supporting material on *Science* Online.
32. O. Tchernichovski, F. Nottebohm, C. E. Ho, B. Pesaran, P. P. Mitra, *Anim. Behav.* **59**, 1167 (2000).
33. S. Deregnaucourt, P. P. Mitra, O. Feher, C. Pytte, O. Tchernichovski, *Nature* **433**, 710 (2005).
34. N. Fujii, A. M. Graybiel, *Science* **301**, 1246 (2003).
35. M. S. Fee, A. A. Kozhevnikov, R. H. Hahnloser, *Ann. N.Y. Acad. Sci.* **1016**, 153 (2004).
36. A. Alvarez-Buylla, C. Y. Ling, F. Nottebohm, *J. Neurobiol.* **23**, 396 (1992).
37. R. Mooney, *J. Neurosci.* **12**, 2464 (1992).
38. R. Mooney, M. Rao, *J. Neurosci.* **14**, 6532 (1994).
39. K. Herrmann, A. P. Arnold, *J. Neurosci.* **11**, 2063 (1991).
40. E. Akutagawa, M. Konishi, *Proc. Natl. Acad. Sci. U.S.A.* **91**, 12413 (1994).
41. J. M. Kittelberger, R. Mooney, *J. Neurosci.* **19**, 9385 (1999).
42. L. L. Stark, D. J. Perkel, *J. Neurosci.* **19**, 9107 (1999).
43. G. M. Edelman, *Neural Darwinism: The Theory of Neuronal Group Selection* (Basic Books, New York, 1987).
44. O. Sporns, G. M. Edelman, *Child Dev.* **64**, 960 (1993).
45. P. Marler, *J. Neurobiol.* **33**, 501 (1997).
46. M. Hadders-Algra, *Dev. Med. Child Neurol.* **42**, 566 (2000).
47. We thank A. Graybiel, E. Bizzi, and J. Goldberg for comments on the manuscript and F. Nottebohm for helpful discussion regarding HVC lesions. Supported by NIH grant MH067105, a Hertz Foundation Silvio Micali fellowship (D.A.), and a Friends of the McGovern Institute fellowship (A.S.A.).

Supporting Online Material
www.sciencemag.org/cgi/content/full/320/5876/630/DC1
Materials and Methods
SOM Text
Figs. S1 to S5
Sounds S1 to S6
References

11 January 2008; accepted 24 March 2008
10.1126/science.1155140

High-Thermoelectric Performance of Nanostructured Bismuth Antimony Telluride Bulk Alloys

Bed Poudel,[1,2]* Qing Hao,[3]* Yi Ma,[1,2] Yucheng Lan,[1] Austin Minnich,[3] Bo Yu,[1] Xiao Yan,[1] Dezhi Wang,[1] Andrew Muto,[3] Daryoosh Vashaee,[3] Xiaoyuan Chen,[3] Junming Liu,[4] Mildred S. Dresselhaus,[5] Gang Chen,[3]† Zhifeng Ren[1]†

The dimensionless thermoelectric figure of merit (ZT) in bismuth antimony telluride (BiSbTe) bulk alloys has remained around 1 for more than 50 years. We show that a peak ZT of 1.4 at 100°C can be achieved in a p-type nanocrystalline BiSbTe bulk alloy. These nanocrystalline bulk materials were made by hot pressing nanopowders that were ball-milled from crystalline ingots under inert conditions. Electrical transport measurements, coupled with microstructure studies and modeling, show that the ZT improvement is the result of low thermal conductivity caused by the increased phonon scattering by grain boundaries and defects. More importantly, ZT is about 1.2 at room temperature and 0.8 at 250°C, which makes these materials useful for cooling and power generation. Cooling devices that use these materials have produced high-temperature differences of 86°, 106°, and 119°C with hot-side temperatures set at 50°, 100°, and 150°C, respectively. This discovery sets the stage for use of a new nanocomposite approach in developing high-performance low-cost bulk thermoelectric materials.

Solid-state cooling and power generation based on thermoelectric effects have potential applications in waste-heat recovery, air conditioning, and refrigeration. The efficiency of thermoelectric devices is determined by the materials' dimensionless figure of merit, defined as $ZT = (S^2\sigma/k)T$, where S, σ, k, and T are the Seebeck coefficient, electrical conductivity, thermal conductivity, and absolute temperature, respectively (*1*–*3*). An average ZT in the application temperature range must be higher than 1 to make a thermoelectric device competitive (*1*–*3*).

There have been persistent efforts to improve ZT values since the 1950s, but the peak ZT of dominant commercial materials based on Bi_2Te_3 and its alloys, such as $Bi_xSb_{2-x}Te_3$ (p-type), has remained at 1. During the past decade, several groups have reported enhanced ZT in (i) superlattices such as Bi_2Te_3/Sb_2Te_3 (*4*) and $PbSe_{0.98}Te_{0.02}/PbTe$ (*5*), because of reductions in the lattice thermal conductivity, and (ii) new bulk materials, such as lead antimony silver telluride (LAST) and its alloys (*6*), including skutterudites (*7*). Although high ZT values were reported in superlattice structures, it has proven difficult to use them in large-scale energy-conversion applications because of limitations in both heat transfer and cost. Bulk materials with improved ZT, such as LAST and skutterudites, are ideal for high-temperature operations. However, at relatively near room temperature (0° to 250°C), Bi_2Te_3-based materials still dominate.

We have pursued an approach in which the primary cause of ZT enhancement in superlattices—reduced thermal conductivity—also exists in random nanostructures (*8*, *9*). We report a substantial ZT increase in bulk materials made from nanocrystalline (NC) powders of p-type $Bi_xSb_{2-x}Te_3$, reaching a peak ZT of 1.4 at 100°C. The enhanced ZT is the result of a significant reduction in thermal conductivity caused by strong phonon scattering by interfaces in the nanostructures. There have also been reports of ZT improvements at room temperature in Bi_2Te_3-based materials caused by the addition of Bi_2Te_3 nanotubes (*10*) and by melt spinning (*11*).

Our method, on the other hand, is based on the ball milling and hot pressing of nanoparticles into bulk ingots. This approach is simple, is cost effective, and can be used on other materials. Our materials have a ZT of about 1.2 at room temperature and 0.8 at 250°C with a peak of 1.4 at 100°C. In comparison, conventional Bi_2Te_3-based materials have a peak ZT of about 1 at room temperature and about 0.25 at 250°C. The high ZT in the 25° to 250°C temperature range makes the NC bulk materials attractive for cooling and low-grade waste-heat recovery applications. The materials can also be integrated into segmented thermoelectric devices for thermoelectric power generation that operate at high temperatures. In addition to the high ZT values, the NC bulk materials are also isotropic. They do not suffer from the cleavage problem that is common in traditional zone melting–made ingots, which leads to easier device fabrication and system integration and to a potentially longer device lifetime.

Sample preparation. Nanopowders were made by ball milling bulk p-type BiSbTe alloy ingots (*12*). Bulk disk samples (1.25 to 2.5 cm in diameter and 2 to 15 mm in thickness) were made by hot pressing the nanopowders loaded in 1.25- to 2.5-cm (inner diameter) graphite dies (*12*). Disks (1.25 cm in diameter and 2 mm in thickness) and bars (about 2 mm by 2 mm by

[1]Department of Physics, Boston College, Chestnut Hill, MA 02467, USA. [2]GMZ Energy, Incorporated, 12A Hawthorn Street, Newton, MA 02458, USA. [3]Department of Mechanical Engineering, Massachusetts Institute of Technology (MIT), Cambridge, MA 02139, USA. [4]Laboratory of Solid State Microstructures and Department of Physics, Nanjing University, China. [5]Department of Physics and Department of Electrical Engineering and Computer Science, MIT, Cambridge, MA 02139, USA.

*These authors contributed equally to this work.
†To whom correspondence should be addressed. E-mail: gchen2@mit.edu (G.C.); renzh@bc.edu (Z.R.)

A Specialized Forebrain Circuit for Vocal Babbling in the Juvenile Songbird

Dmitriy Aronov *et al.*

Science **320**, 630 (2008);
DOI: 10.1126/science.1155140

Science (print ISSN 0036-8075; online ISSN 1095-9203) is published weekly, except the last week in December, by the American Association for the Advancement of Science, 1200 New York Avenue NW, Washington, DC 20005.